benzene ring; Elderfied, R. C. *Heterocyclic Chemistry*; Elderfied, R. C. ed.; Wiley: New York, 1957; Vol. 5, 171.
5. Huisgen, R.; Nakaten, H. *Ann. Chem.* **1951**, *573*, 181.
6. (a) Smith, H. *J. Chem. Soc.* **1953**, 803; (b) Rogers, N. A.; Smith, H. *J. Chem. Soc.* **1955**, 341; (c) Akherm, A. A.; Lakhvich, F. A.; Budai, S. I.; Khlebnicova, T. S.; Peterusevich, I. I. *Synthesis* **1978**, 925.
7. Phenylhydrazine and other hydrazines are also reacted with **1** to afford 1-substituted 4-oxo-4,5,6,7-tetrahydroindazoles over 85% yields.
8. All new compounds were fully characterized by spectroscopic methods as well as elemental analysis. **4-Oxo-3-phenyl-4,5,6,7-tetrahydroindazole (2b)**: Colorless plates (89%), mp. 193-194℃; IR (KBr) ν 3160, 3080, 2920, 1580, 1550, 1430, 1350, 1310, 1260, 1165, 1125, 1060, 1015, 970, 890, 775, 745, 690 cm^{-1}; ^{1}H-NMR ($CDCl_3$ in DMSO-d_6, 300 MHz) δ 2.08 (quintet, 2H, J=6.2 Hz), 2.45 (t, 2H, J=6.2 Hz), 2.85 (t, 2H, J=6.2 Hz), 7.37 (m, 3H), 8.05 (m, 2H), 13.20 (br.s, NH); ^{13}C-NMR ($CDCl_3$ in DMSO-d_6, 75.5 MHz) δ 21.3, 25.6, 36.3, 119.3, 127.1, 127.7, 131.3, 132.0, 164.8, 165.6, 195.9. **4-Hydroxy-3-phenyl-4,5,6,7-tetrahydroindazole (3b)**: Colorless platelets (85%), mp. 212-214℃; IR (KBr) ν 3170-3100, 3050, 2910-2880, 1430, 1390, 1330, 1265, 1150, 1095, 1050, 980, 945, 865, 830, 755, 725, 690 cm^{-1}; ^{1}H-NMR ($CDCl_3$ in DMSO-d_6, 300 MHz) δ 1.69-1.79 (m, 2H), 1.95-2.09 (m, 2H), 2.47-2.58 (m, 1H), 2.75 (dt, 1H, J=16, 4.5 Hz), 4.60 (d, J=6.0 Hz, H_4), 4.79 (t, 1H, J=5.4 Hz), 7.26 (t, 1H, J=7.5 Hz), 7.37 (t, 2H, J=7.5 Hz), 7.97 (dm, 2H, J=7.5 Hz), 12.40 (br.s, NH); ^{13}C-NMR ($CDCl_3$ in DMSO-d_6, 75.5 MHz) δ 16.6, 32.9, 39.5, 60.2, 78.3, 108.2, 115.0, 126.4, 126.6, 127.9, 130.8, 137.1, 150.3. **3-Phenyl-6,7-dihydroindazole (4b)**: Pale yellow oil (98%). IR (thin film) ν 3150, 3090, 3030, 2920, 1685, 1600, 1485, 1425, 1310, 1210, 1130, 1065, 1005, 975, 910, 860, 780, 760, 725, 690, 665 cm^{-1}; ^{1}H-NMR ($CDCl_3$, 300 MHz) δ 2.36-2.43 (m, 2H, H_6), 2.73 (td, 2H, J=8.3, 1.8 Hz, H_7), 5.78 (dt, J=9.7, 4.3 Hz, H_5), 6.64 (dt, J=9.7, 2.1 Hz, H_4), 7.35 (m, 3H), 7.57 (m, 2H), 10.55 (br.s, NH); ^{13}C-NMR ($CDCl_3$, 75.5 MHz) δ 20.9, 23.6, 113.1, 119.7, 124.0, 126.9, 127.8, 128.7, 130.8, 139.1, 148.0. Anal. Calcd. for $C_{13}H_{12}N_2$ C: 79.56, H: 6.16, N: 14.27; Found C: 79.63, H: 6.17, N: 14.29. **3-Isopypylindazole (5a)**: Colorless platelets (93%), mp. 103-104℃ (lit.[10]: 102-104℃). Unreported spectral data are: IR (KBr) ν 3060, 2950, 1605, 1570, 1525, 1480, 1440, 1355, 1290, 1225, 1165, 1140, 1115, 1095, 1060, 1040, 990, 900, 785, 760, 730 cm^{-1}; ^{1}H-NMR ($CDCl_3$, 300 MHz) δ 1.47 (d, 6H, J=7.0 Hz), 3.45 (septet, 1H, J=7.0 Hz), 7.08 (t, 1H, J=8.0 Hz), 7.33 (m, 2H), 7.75 (d, 1H), 11.05 (br., NH); ^{13}C-NMR ($CDCl_3$, 75.5 MHz) δ 22.1, 27.8, 109.9, 119.8, 120.6, 121.1, 126.4, 141.5, 151.8, **3-Phenylindazole (5b)**: Colorless crystals (96%), mp. 110-112℃ (lit.[11]; 106-107℃). Unreported spectral data are as follows: IR (KBr) ν 3120, 3050, 1595, 1530, 1465, 1325, 1245, 1120, 1090, 1060, 1020, 995, 980, 895, 765, 725, 685 cm^{-1}; ^{1}H-NMR ($CDCl_3$, 300 MHz) δ 7.11 (d, 1H, J=8.1 Hz), 7.20 (t, 1H, J=8.1 Hz), 7.31 (td, 1H, J=8.1, 1.8 Hz), 7.48 (td, 1H, J=7.5, 2.1 Hz), 7.56 (td, 2H, J=7.6, 1.0 Hz), 8.05 (d, 1H, J=8.1 Hz), 8.07 (dd, 2H, J=8.1, 1.2 Hz), 12.40 (br.s, NH); ^{13}C-NMR ($CDCl_3$, 75.5 MHz) δ 110.5, 120.9, 121.2, 126.6, 127.8, 128.1, 129.0 (2 C's), 133.6, 141.7, 145.5. **3-(4-Fluorophenyl)indazole (5c)**: Colorless platelets (95%), mp. 135-136℃. IR (KBr) ν 3100, 1590, 1470, 1400, 1325, 1205, 1145, 1125, 1090, 990, 900, 835, 810, 770, 730 cm^{-1}; ^{1}H-NMR ($CDCl_3$, 300 MHz) δ 7.19 (m, 4H), 7.31 (dd, 1H, J=8.4, 7.0 Hz), 7.95 (m, 3H), 12.04 (br.s, NH); ^{13}C-NMR ($CDCl_3$, 75.5 MHz) δ 110.3, 116.0 (d, $^2J_{C\text{-}F}$=22 Hz), 120.8, 121.4, 126.9, 129.4 (d, $^3J_{C\text{-}F}$=8 Hz), 129.6, 129.7, 141.7, 144.7, 162.9 (d, $^1J_{C\text{-}F}$=256 Hz). Anal. Calcd. for $C_{13}H_9N_2F$ C: 73.57, H: 4.27, N: 13.20; Found C: 73.63, H: 4.28, N: 13.17. **3-Benzylindazole (5d)**: Colorless platelets (94%), mp. 115-116℃. IR (KBr) ν 3125, 2920, 2860, 1590, 1480, 1440, 1420, 1360, 1330, 1245, 1170, 1140, 1105, 1060, 1025, 990, 930, 890, 735, 715, 690 cm^{-1}; ^{1}H-NMR ($CDCl_3$, 300 MHz) δ 4.37 (s, methylene H), 7.01 (m, 1H), 7.22 (m, 7H), 7.49 (d, 1H), 11.35 (br., NH); ^{13}C-NMR ($CDCl_3$, 75.5 MHz) δ 33.6, 109.9, 120.3, 120.4, 122.1, 126.3, 126.6, 128.4, 128.7, 139.0, 141.4, 145.6. Anal. Calcd. for $C_{14}H_{12}N_2$ C: 80.74, H: 5.81, N: 13.45; Found C: 80.66, H: 5.84, N: 13.50.
9. Rinehart, K. L.; Perkins, E. G. *Org. Syn., Coll. Vol. IV* **1963**, 444.
10. Hannig, E.; Kollmorgan, C. H. R.; Korner, M. *Pharmazie* **1976**, *31*, 534.
11. Rüchardt, C.; Hassmann, V. *Liebigs Ann. Chem.* **1980**, 908.

A Substituent Effect on the Palladium(II) Catalyzed [3,3]-Sigmatropic Rearrangement of Allylic Esters

Ki-Whan Chi* and Eon-Chul Koo

Department of Chemistry, University of Ulsan, 680-749

Received July 29, 1993

[3,3]-Sigmatropic rearrangements which are represented by Cope[1] and Claisen[2] rearrangements have been applied for pivotal steps in the syntheses of complex molecules. By taking advantage of the stereospecificity and peculiarity of those synthetic methodologies, we recently completed the total syntheses of natural products, (+)-costunolide, dihydroreynosin and dihydrosantamarine, *via* tandem Cope-Claisen rearrangement.[3] In spite of the usefulness of [3,3]-sigmatropic rearrangements in organic synthesis, the required high reaction temperature could be a major drawback for most [3,3]-sigmatropic rearrangements except Ireland-Claisen type[4]. For example, Cope rearrangement usually occurs at higher than 150℃ so that its applicability has been restricted to thermally stable precursors.[5] One reasonable way to circumvent this problem might be the use of catalytic pathway and various catalysts[6], which make [3,3]-sigmatropic rearrangements undergo under mild conditions, have been developed. However, only few of systematic studies[7] have been executed to elucidate the catalytic pathway and much of the reaction mechanism for [3,3]-sigmatropic rearrangements has not been cleared thus far. Allylic ester rearrangement[8], one of

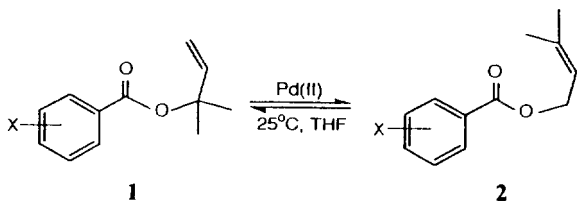

1 **2**

Scheme 1.

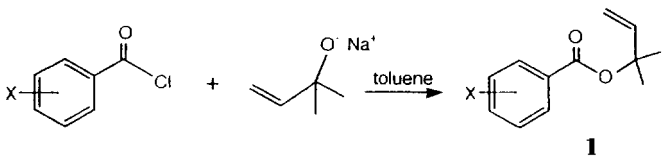

1

1a; X= p-CH_3O **1b**; X= p-CH_3 **1c**; X= H **1d**; X= p-Cl
1e; X= p-Br **1f**; X= m-F **1g**; X= m-Br **1h**; X= m-CF_3
1i; X= p-CF_3 **1j**; X= m-NO_2 **1k**; X= p-NO_2

Scheme 2.

the [3,3]-sigmatropic rearrangements, has turned out to be effectively catalyzed by Pd(II)[9] and it has been successfully applied for the formation of key intermediate in organic synthesis.[10] Also, a catalytic reaction mechanism of allylic ester rearrangement has been proposed and discussed without any quantitative kinetic study.[7(a),(b)]

In this paper, we would like to report for the first time a substituent effect on the Pd(II) catalyzed allylic ester rearrangement of 1,1-dimethyl-2-propenyl benzoate (Scheme 1). We hoped that this quantitative outcome could give us some insight for the structure of transition state and detail of reaction mechanism.

Since the equilibrium of catalytic ester rearrangement in Scheme 1 was expected to be shifted in favor of the product[11] (tri-substituted alkene and 1° benzoate), the various substrates **1a-k** were prepared as shown in Scheme 2. The substrates **1a-k** were purified by flash chromatography[12] and characterized by ^{1}H-NMR, IR and MS.

To the pre-equilibrated 5.0-6.0$\times10^{-2}$ M solution of substrate **1** in 10 m*l* dry THF at 25.0± 0.1℃ was added 0.01-0.02 equivalent of bis(acetonitrile)palladium(II)chloride and the quantity of residual substrate **1** was analyzed every 10-15 minutes by gas chromatography.[13] Some of the substrates which were injected into GC might be supposed to undergo thermal rearrangement, but the rate of vapour-phase thermal rearrangement was relatively slow enough for the determination of the rate constant of liquid-phase catalyzed rearrangement.[14] All the catalytic reactions were completed within 1-8 hours and the formation of thermodynamically more stable products **2a-k** was favored in more than 97% GC yield. Spectral data of rearranged products were consistent with the assigned structures **2a-k**. Pseudo-first order rate constant was obtained by least-square method from the slope of substrate concentration versus time. Pseudo-first order plots were linear (correlation coefficients>0.990) over more than two half-lives.

The second-order rate constant was then calculated from a division of the pseudo first-order rate constant by the concentration of catalyst (Table 1).

A Hammett plot between these second-order rate constants and σ is outlined in Figure 1. It shows a good linear correlation (correlation coefficient=0.977) and retardation of the reaction rate is directly proportional to the strength of electron-withdrawing capability of substituents (ρ= −1.05).

Table 1. The second-order rate constants

Substrate	Substituent X	Number of runs	[catalyst] M×10^4	k_x min^{-1} M^{-1}	σ^{15}
1a	*p*-CH_3O	3	5.10-5.67	130.± 5	−0.28
1b	*p*-CH_3	3	5.39-5.78	92.9± 2.0	−0.14
1c	H	5	5.39-5.78	63.2± 8.5	0
1d	*p*-Cl	3	6.17-6.55	53.1± 4.6	0.24
1e	*p*-Br	3	5.96-6.94	46.2± 1.6	0.26
1f	*m*-F	5	5.61-6.55	28.5± 4.0	0.34
1g	*m*-Br	4	5.78-6.31	32.8± 2.2	0.37
1h	*m*-CF_3	4	6.17-6.94	17.7± 0.9	0.46
1i	*p*-CF_3	2	6.94-7.02	19.4± 0.1	0.53
1j	*m*-NO_2	3	5.78-7.25	10.1± 1.6	0.71
1k	*p*-NO_2	3	6.17-6.94	11.1± 1.3	0.81

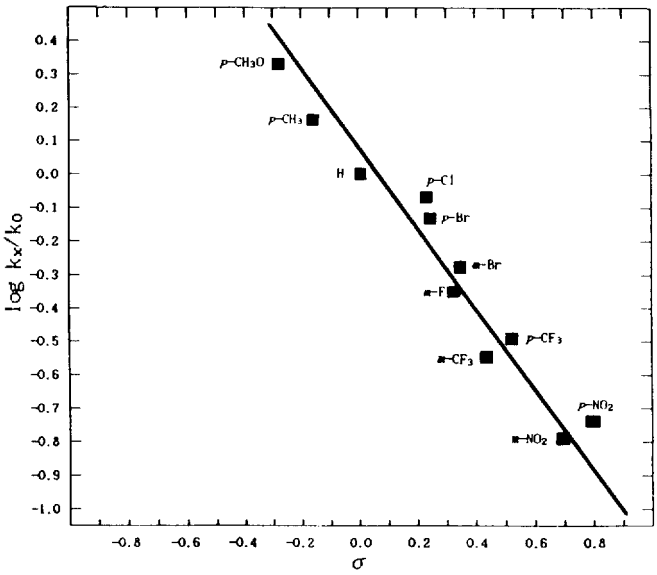

Figure 1. Hammett plot of log k_x/k_H *vs* σ.

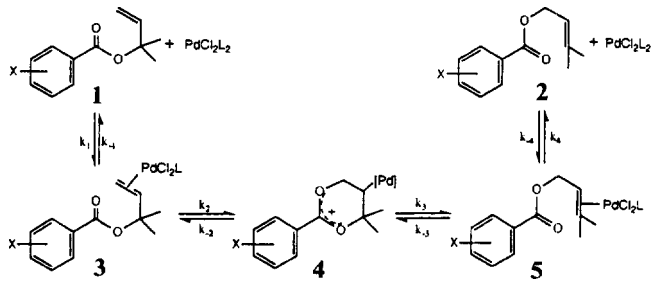

1 **2** **3** **4** **5**

Scheme 3.

The experimental result supports a cyclization-induced rearrangement mechanism as shown in Scheme 3.

Since the rate of rearrangement decreases proportional to the substituent constant σ, the rate-determining step is believed to be the second step in which the positive-charged

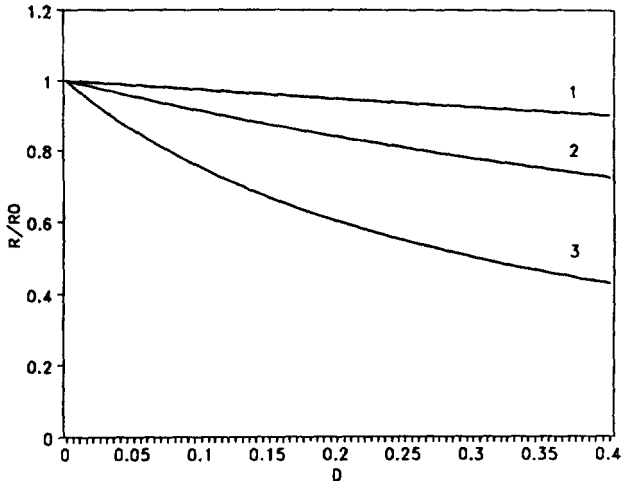

Figure 4. The ratio of R/R_0 for the bistable system with $\nu=0.2$. The curves 1, 2, and 3 correspond to $\mu=0.5$, $\mu=1$, and $\mu=2$, respectively.

and $\nu=0.9$, respectively. In Figure 4 we have taken μ to be 0.5, 1, and 2, respectively, when $\nu=0.2$. As D increases the ratio in large μ value decreases faster than the ratio in small μ does. As shown in Figure 3, it is obvious that in the region $\nu<1$ the transition rates decrease with increasing D. As the exponent ν increases, the transition rates decrease and relaxation times increase. In the limit $\nu\rightarrow1$, the transition rate approaches zero.

In the result, in the region for which $\nu<1$ the transition rates decrease as ν increases and ν decreases shown in Figure 3 and 4. However, in the case that $\nu>1$, it is obvious that in Eq. (17) never probability can be reach $y\rightarrow\infty$ in any finite time. It means that the system cannot be reach the unstable state since the concentration $x\rightarrow0$ (unstable point) corresponds to $y\rightarrow\infty$. When $\nu>1$ the random force is so weak that the system is entirely controlled by the deterministic term in the vicinity of the unstable state. The transition between the two deterministic stable states cannot occur and the initial distribution is continuously retained.

References

1. I. L'Hereux and R. Kapral, *J. Chem. Phys.* **88**, 1768 (1988).
2. C. Van den Broeck and P. Hnggi, *Phys. Rev.* **A30**, 2730 (1984).
3. J. M. Porra, J. Masoliver, and K. Lindenberg, *Phys. Rev.* **A44**, 4866 (1991); J. Masoliver, B. West, and K. Lindenberg, *ibid.*, **35**, 3086 (1987).
4. G. Hu and K. He, *Phys. Rev.* **A45**, 5447 (1992).
5. H. Risken, *The Fokker-Planck Equation*, Spinger-Velag, New York, 1984.
6. M. Kus, E. Wajnryb, and K. Wodkiewicz, *Phys. Rev.* **A43**, 4167 (1991).
7. P. Glansdorff and I. Prigogine, *Thermodynamic Theory of Structure, Stability, and Fluctuations*, Wiley-Interscience, New York, 1971.
8. R. J. Field and M. Burger, *Oscillations and Traveling Waves in Chemical Systems*, John Wiley & Sons, New York, 1974.
9. G. Nicolis and I. Prigogine, *Self-Organization in Non-equilibrium System*, John Wiley and Sons, New York, 1977.
10. F. Schlögl, *Z. Phys.* **248**, 446 (1971); **253**, 147 (1972).
11. C. J. Kim, D. J. Lee, and K. J. Shin, *Bull. Korean Chem. Soc.*, **11**, 557 (1990).
12. D. Chandler, *J. Chem. Phys.* **68**, 2959 (1978).
13. M. Abramowitz and I. A. Stegun, *Hanbook of Mathematical functions*, Natl. Bureau of Standards, 1965.
14. A. Nitzan, P. Ortoveva, J. Deutch, and J. Ross, *J. Chem. Phys.* **61**, 1056 (1974).
15. I. Procaccia and J. Ross, *J. Chem. Phys.* **67**, 5558 (1977).

Orbital Interactions in BeC_2H_2 and LiC_2H_2 Complexes

Ikchoon Lee* and Jae Young Choi

Department of Chemistry, Inha University, Inchon 402-751. *Received August 17, 1992*

Ab initio calculations are carried out at the 6-311G** level for the C_{2v} interactions of Be and Li atoms with acetylene molecule. The main contribution to the deep minima on the $^3B_2$ BeC_2H_2 and $^2B_2$ LiC_2H_2 potential energy curves is the b_2 $(2p(3b_2)-|\pi_g^*(4b_2))$ interaction, the a_1 $(2s(6a_1)-|\pi_u(5a_1))$ interaction playing a relatively minor role. The exo deflection of the C-H bonds is basically favored, as in the b_2 interaction, due to steric crowding between the metal and H atoms, but the strong in-phase orbital interaction, or mixing, of the a_1 symmetry hydrogen orbital with the $5a'_1$, $6a'_1$ and $7a'_1$ orbitals can cause a small endo deflection in the repulsive complexes. The Be complex is more stable than the Li complex due to the double occupancy of the 2*s* orbital in Be. The stability and structure of the MC_2H_2 complexes are in general determined by the occupancy of the singly occupied frontier orbitals.

Introduction

The interactions of metal atoms with molecules have been the subject of many experimental and theoretical studies.[1] The main purpose of the research in this field is a fundamental understanding of catalysis. It has been suggested that